Identification of Piezomicropositioning Hammerstein Systems with Generalized Prandtl-Ishlinskii Hysteresis Nonlinearities

Khaled F. Aljanaideh, Mohammad Al Janaideh, Micky Rakotondrabe, and Deepa Kundur

***Abstract*— We introduce an algorithm to identify the nonlinear dynamics of a class of smart micropositioning systems, which is modeled as a Hammerstein system, that is, a cascade of a generalized Prandtl-Ishlinskii (GPI) hysteresis nonlinearity with a linear dynamic system. The GPI hysteresis nonlinearity, the linear dynamic system, and the intermediate signal between them are assumed to be unknown. The first stage in the algorithm is to identify the linear dynamic plant from measurements of the input and output of the Hammerstein system. Then, the unknown intermediate signal is reconstructed using the output and the identified model of the linear system. Finally, the GPI nonlinearity is estimated using the input and the reconstructed intermediate signal.**

I. Introduction

Smart positioning actuators, such as piezoelectric and magnetostrictive actuators, are considered an attractive choice for micro-positioning applications where fast response (milliseconds) with high resolution (nanometers) is desired. These actuators have been used in motion control applications to deliver fast output displacement in the micro/nano level in response to the applied inputs (voltage or current inputs) [1]. However, the advantages of smart positioning actuators come with the hysteresis nonlinearities in the output displacement. These nonlinearities cause oscillations and inaccuracies with positioning errors if not correctly considered [2]–[4]. Then, it is essential to characterize the nonlinear dynamics of these smart actuators in order to propose control techniques that can reduce the positioning errors. The dynamics of smart positioning actuators can be characterized by a Hammerstein system, that is, a cascade of a hysteresis nonlinearity and a linear dynamic system, see for example [5]–[7]. Different models have been used to model hysteresis nonlinearties such as the Preisach model, generalized Prandtl-Ishlinskii (GPI) model, Duhem model, and Bouc-Wen model.

The GPI model has been recently used in different precision motion studies to model: (i) voltage-to-displacement hysteresis loops of piezoelectric actuators, and (ii) current-to-displacement hysteresis loops of magnetostrictive actuators [8]. The GPI model is constructed with a fewer number of parameters than operator-based hysteresis models, and the inverse model can be obtained analytically [8]. In this study, we consider a Hammerstein system to model the nonlinearity and the dynamics of smart-material based actuators. This Hammerstein system has been used to model different smart material-based actuators, see for example [5], [9].

Identification of Hammerstein systems has been studied in the literature [10]–[16]. However, most of studies consider Hammerstein systems with memeoryless nonlinearities. Identification of Hammerstein systems in the presence of hysteresis-backlash and hysteresis-relay nonlinearities was studied in [17]. However, hysteresis-backlash and hysteresis-relay nonlinearities cannot describe hysteresis nonlinearities that appear in smart positioning actuators. In [3], pseudo random binary sequences was used to identify the linear dynamic part only of the piezoelectric actuator, while in [18] neural networks were used to identify a hysteretic piezoelectric robotic micro-manipulator.

In this paper, we consider the problem of identifying Hammerstein systems with GPI hysteresis nonlinearities. This work extends the results in [19], where Hammerstein systems with Prandtl-Ishlinskii (PI) hysteresis nonlinearities were considered. We assume that only the input and output of the Hammerstein system are known, where the intermediate signal of the Hammerstein system is inaccessible. The first stage in the algorithm is to identify the linear plant from measurements of the input and output of the Hammerstein system. Then, the unknown intermediate signal in the Hammerstein system is reconstructed using the output and the identified model of the linear part of the Hammerstein system. Finally, the hysteresis nonlinearity is estimated using the input and the reconstructed intermediate signal.

II. The Hammerstein system with the GPI Model

This section presents the Hammerstein system that characterizes the dynamics of a class of smart material-based actuators such as piezoelectric and magnetostrictive actuators, see [2], [7], [20].

A. The Hammerstein system

Consider the discrete-time SISO Hammerstein system shown in Figure 1, where u is the input, $\mathcal{P}_{\mathcal{D}} : \mathbb{R} \to \mathbb{R}$ is the GPI hysteresis nonlinearity, v is the intermediate signal, and y is the output of the asymptotically stable, SISO, linear, time-invariant, discrete-time system G. This approach has been used in different studies to model the dynamics of smart material-based actuators, see for example [3], [5], [9].

K. Aljanaideh is with the Department of Aeronautical Engineering, Jordan University of Science and Technology, Irbid, Jordan 22110, kfaljanaideh@just.edu.jo

M. Al Janaideh is with the Department of Mechanical Engineering, Memorial University of Newfoundland, St John's, Newfoundland A1B 3X5, Canada, maljanaideh@mun.ca.

M. Rakotondrabe is with the Department of Automatic Control and Micro-Mechatronic Systems, FEMTO-ST, AS2M, Univ. Bourgogne Franche-Comté, Univ. de Franche-Comt/CNRS/ENSMM/UTBM, FEMTO-ST Institute, Besançon France, mrakoton@femto-st.fr

D. Kundur is with the Department of Electrical and Computer Engineering, University of Toronto, Toronto, Ontario M5S 2E4, Canada, dkundur@ece.utoronto.ca.

It is important to mention that the time-invariant discrete-time system G represents the linear dynamics of the actuator, and vibrations [21]. The creep can be as well approximated by a linear behavior enclosed in G, though it is initially a nonlinear phenomenon [22].

B. The hysteresis model

The GPI hysteresis model has been used to model nonlinearties in the output displacement of piezoelectric and magnetostrictive actuators [7], [23]. This model is constructed based on a linear combination of play hysteresis operators. For all $k \geq 0$, the output v of the GPI model is

$$v(k) \triangleq \mathcal{P}_{\mathcal{D}}[u](k) = \mathcal{P} \circ \mathcal{D}[u](k), \tag{1}$$

where $\mathcal{D}[u](k)$ is a memoryless model constructed with deadzone operators $\mathcal{Z}_{\eta_i}$ as

$$\mathcal{D}[u](k) \triangleq \sum_{i=1}^{m} g_i \mathcal{Z}_{\eta_i}[u](k), \tag{2}$$

where m is the number of deadzone operators, $g_1, \ldots, g_m$ are positive weights, $\eta_1, \ldots, \eta_m$ are positive constants represent thresholds of the deadzone operators. For convenience, we define $z(k) \triangleq \mathcal{D}[u](k)$ and $z_i(k) \triangleq \mathcal{Z}_{\eta_i}[u](k)$. Then,

$$z_i(k) = \begin{cases} u(k) - \eta_i, \; u(k) > u(k-1) \text{ and } u(k) > \eta_i, \\ u(k) + \eta_i, \; u(k) < u(k-1) \text{ and } u(k) < -\eta_i, \\ 0, \quad \text{otherwise}, \end{cases} \tag{3}$$

which can be written as

$$z_i(k) = u(k) + R_{\eta_i}(k), \tag{4}$$

where

$$R_{\eta_i}(k) \triangleq \begin{cases} -\eta_i, & u(k) > u(k-1) \text{ and } u(k) > \eta_i, \\ \eta_i, & u(k) < u(k-1) \text{ and } u(k) < -\eta_i \\ -u(k), & \text{otherwise}. \end{cases} \tag{5}$$

Therefore,

$$\begin{aligned} z(k) &= \sum_{i=1}^{m} g_i z_i(k) \\ &= \sum_{i=1}^{m} g_i (u(k) + R_{\eta_i}(k)) \\ &= \sum_{i=1}^{m} g_i u(k) + \sum_{i=1}^{m} g_i R_{\eta_i}(k). \end{aligned} \tag{6}$$

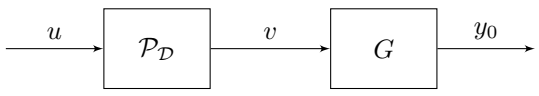

Fig. 1. Hammerstein System with the GPI hysteresis model and the linear time-invariant discrete-time system G. In this systems, u is the input, $\mathcal{P}_{\mathcal{D}}$ is the hysteresis nonlinearity, v is the unknown intermediate signal, and y is the output.

For all $i = 1, \ldots, n$, let $\mathcal{F}_{r_i}$ denote a hysteresis play operator with threshold $r_i > 0$. Then, $\mathcal{F}_{r_i}$ can be expressed as

$$\mathcal{F}_{r_i}[z](k) = \max\{z(k) - r_i, \min\{z(k) + r_i, \mathcal{F}_{r_i}[z](k-1)\}\}, \tag{7}$$

which is also equivalent to

$$\mathcal{F}_{r_i}[z](k) = \tag{8}$$
$$\begin{cases} z(k) + r_i, \; z(k) < z(k-1) \text{ and } z(k) + r_i < \mathcal{F}_{r_i}[z](k-1), \\ z(k) - r_i, \; z(k) > z(k-1) \text{ and } z(k) - r_i > \mathcal{F}_{r_i}[z](k-1), \\ \mathcal{F}_{r_i}[z](k-1), \; \text{otherwise}. \end{cases}$$

Note that (8) can be written as

$$\mathcal{F}_{r_i}[z](k) = z(k) + q_i[z](k), \tag{9}$$

where

$$q_i[z](k) \triangleq \tag{10}$$
$$\begin{cases} r_i, & z(k) < z(k-1) \text{ and } z(k) + r_i < \Gamma_{r_i}[z](k-1), \\ -r_i, & z(k) > z(k-1) \text{ and } z(k) - r_i > \Gamma_{r_i}[z](k-1), \\ \mathcal{F}_{r_i}[z](k-1) - z(k), & \text{otherwise}. \end{cases}$$

The output v of the GPI model can be written as

$$v(k) \triangleq \sum_{i=1}^{n} p_i \mathcal{F}_{r_i}[z](k), \tag{11}$$

where for all $i = 1, \ldots, n$, p_i are positive weights. Then, using (6) and (9), (11) becomes

$$\begin{aligned} v(k) &= \sum_{i=1}^{n} p_i (z(k) + q_i[z](k)) \\ &= \sum_{i=1}^{n} p_i z(k) + \sum_{i=1}^{n} p_i q_i[z](k) \\ &= \sum_{i=1}^{n} p_i \sum_{j=1}^{m} g_j u(k) + \sum_{i=1}^{n} p_i \sum_{j=1}^{m} g_j R_{\eta_j}(k) + \sum_{i=1}^{n} p_i q_i[z](k) \\ &= \left(\sum_{i=1}^{n} p_i \sum_{j=1}^{m} g_j \right) u(k) + \rho(k) \\ &= \alpha u(k) + \rho(k), \end{aligned} \tag{12}$$

where

$$\alpha \triangleq \sum_{i=1}^{n} p_i \sum_{j=1}^{m} g_j \in \mathbb{R}, \tag{13}$$

$$\rho(k) \triangleq \sum_{i=1}^{n} p_i \sum_{j=1}^{m} g_j R_{\eta_j}(k) + \sum_{i=1}^{n} p_i q_i[z](k). \tag{14}$$

For all $j \geq 0$, let H_j denote the jth Markov (impulse response) parameter of G. Then, y_0 can be written as [24]

$$y_0(k) = \sum_{j=0}^{\infty} H_j v(k-j). \tag{15}$$

Moreover, using (12), (15) can be written as

$$y_0(k) = \sum_{j=0}^{\infty} H_j(\alpha u(k-j) + \rho(k-j))$$
$$= \alpha \sum_{j=0}^{\infty} H_j u(k-j) + \sum_{j=0}^{\infty} H_j \rho(k-j). \quad (16)$$

III. Identification of the Linear Part of the Hammerstein System

Consider the FIR model of G given by [24]

$$G_\mu(\mathbf{q}) \triangleq \sum_{i=0}^{\mu} H_i \mathbf{q}^{-i}, \quad (17)$$

where $\mu \geq 0$ is the order of $\hat{G}_\mu$, $\mathbf{q}^{-1}$ is the backward shift operator, and for all $i = 0, \ldots, \mu$, H_i is the ith Markov parameter of G.

For all $k \geq 0$, (15) can be written as

$$y_0(k) = y_{0,\mu}(k) + e_\mu(k), \quad (18)$$

where

$$y_{0,\mu}(k) \triangleq \sum_{j=0}^{\min\{\mu,k\}} H_j v(k-j), \quad (19)$$

$$e_\mu(k) \triangleq y_0(k) - y_{0,\mu}(k) \quad (20)$$

are the output of the FIR model (17) of G, and the error in the output of the FIR model at time k. Taking the limit of (19) as μ tends to infinity, and using (16) yields, for all $k \geq 0$,

$$\lim_{\mu\to\infty} y_{0,\mu}(k) = \sum_{j=0}^{k} H_j v(k-j) = y_0(k). \quad (21)$$

Therefore, for all $k \geq 0$,

$$\lim_{\mu\to\infty} e_\mu(k) = y_0(k) - \lim_{\mu\to\infty} y_{0,\mu}(k) = 0. \quad (22)$$

Consider the identification problem shown in Figure 2, where u is a deterministic signal that is persistently exciting of a sufficient order, w is a realization of a zero-mean, stationary, white, ergodic, Gaussian random process $\mathcal{W}$, and the intermediate signal v is unknown.

Note that (18) can be expressed as

$$y_0(k) = \theta_\mu \phi_v(k) + e_\mu(k), \quad (23)$$

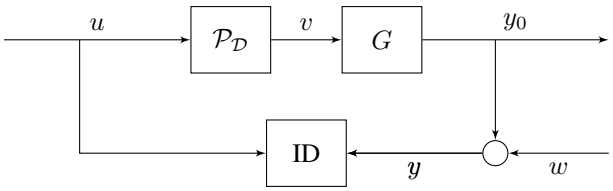

Fig. 2. Identification of the Hammerstein system, where $\mathcal{P}_\mathcal{D}$ is the GPI hysteresis nonlinearity, G is a linear system, u is the applied input, y is the measured output, w is the output sensor noise, and v is the unknown intermediate signal.

where

$$\theta_\mu \triangleq \begin{bmatrix} H_0 & \cdots & H_\mu \end{bmatrix},$$
$$\phi_v(k) \triangleq \begin{bmatrix} v(k) & \cdots & v(k-\mu) \end{bmatrix}^{\mathrm{T}}.$$

Moreover, for all $k \geq 0$

$$y(k) = \theta_\mu \phi_v(k) + w(k) + e_\mu(k). \quad (24)$$

The least squares estimate $\hat{\theta}_{\mu,\ell}$ of θ_μ is given by

$$\hat{\theta}_{\mu,\ell} = \arg\min_{\bar{\theta}_\mu} \left\| \Psi_{y,\ell} - \bar{\theta}_\mu \Phi_{\mu,\ell} \right\|_{\mathrm{F}}, \quad (25)$$

where $\bar{\theta}_\mu \in \mathbb{R}^{1\times(\mu+1)}$,

$$\Psi_{y,\ell} \triangleq \begin{bmatrix} y(\mu) & \cdots & y(\ell) \end{bmatrix},$$
$$\Phi_{\mu,\ell} \triangleq \begin{bmatrix} \phi_\mu(\mu) & \cdots & \phi_\mu(\ell) \end{bmatrix},$$
$$\phi_\mu(k) \triangleq \begin{bmatrix} u(k) & \cdots & u(k-\mu) \end{bmatrix}^{\mathrm{T}},$$

and ℓ is the number of samples.

The eigensystem realization algorithm (ERA), which is based on the Ho-Kalman realization theory, can be used to construct a transfer function estimate of G from the estimated Markov parameters $\hat{\theta}_{\mu,\ell}$ [25], [26].

IV. Consistency Analysis

It follows from (25) that the least squares estimate $\hat{\theta}_{\mu,\ell}$ of θ_μ satisfies

$$\Psi_{y,\ell}\Phi_{\mu,\ell}^{\mathrm{T}} = \hat{\theta}_{\mu,\ell}\Phi_{\mu,\ell}\Phi_{\mu,\ell}^{\mathrm{T}}. \quad (26)$$

Moreover, it follows from (24) that

$$\Psi_{y,\ell} = \theta_\mu \Phi_{v,\ell} + \Psi_{w,\ell} + \Psi_{e_\mu,\ell}, \quad (27)$$

where

$$\Phi_{v,\ell} \triangleq \begin{bmatrix} \phi_v(\mu) & \cdots & \phi_v(\ell) \end{bmatrix}, \quad (28)$$
$$\Psi_{w,\ell} \triangleq \begin{bmatrix} w(\mu) & \cdots & w(\ell) \end{bmatrix}, \quad (29)$$
$$\Psi_{e_\mu,\ell} \triangleq \begin{bmatrix} e_\mu(\mu) & \cdots & e_\mu(\ell) \end{bmatrix}. \quad (30)$$

Using (27), (26) becomes

$$(\theta_\mu \Phi_{v,\ell} + \Psi_{w,\ell} + \Psi_{e_\mu,\ell})\Phi_{\mu,\ell}^{\mathrm{T}} = \hat{\theta}_{\mu,\ell}\Phi_{\mu,\ell}\Phi_{\mu,\ell}^{\mathrm{T}}. \quad (31)$$

Using (12), note that for all $k \geq 0$,

$$\phi_v(k) = \alpha\phi_\mu(k) + \phi_\rho(k), \quad (32)$$

where

$$\phi_\rho(k) \triangleq \begin{bmatrix} \rho(k) & \cdots & \rho(k-\mu) \end{bmatrix}^{\mathrm{T}}. \quad (33)$$

Therefore, using (32) we can write

$$\Phi_{v,\ell} = \alpha\Phi_{\mu,\ell} + \Phi_{\rho,\ell}, \quad (34)$$

where

$$\Phi_{\rho,\ell} \triangleq \begin{bmatrix} \phi_\rho(\mu) & \cdots & \phi_\rho(\ell) \end{bmatrix}. \quad (35)$$

Then, using (34), (31) can be written as

$$\alpha\theta_\mu\Phi_{\mu,\ell}\Phi_{\mu,\ell}^{\mathrm{T}} + \theta_\mu\Phi_{\rho,\ell}\Phi_{\mu,\ell}^{\mathrm{T}} + \Psi_{w,\ell}\Phi_{\mu,\ell}^{\mathrm{T}} + \Psi_{e_\mu,\ell}\Phi_{\mu,\ell}^{\mathrm{T}}$$
$$= \hat{\theta}_{\mu,\ell}\Phi_{\mu,\ell}\Phi_{\mu,\ell}^{\mathrm{T}}. \quad (36)$$

Since w is a realization of a stationary ergodic random process, then dividing (36) by ℓ and taking the limit as ℓ tends to infinity yields

$$\alpha\theta_\mu \lim_{\ell\to\infty} \frac{1}{\ell}\Phi_{\mu,\ell}\Phi_{\mu,\ell}^{\mathrm{T}} + \theta_\mu \lim_{\ell\to\infty} \frac{1}{\ell}\Phi_{\rho,\ell}\Phi_{\mu,\ell}^{\mathrm{T}} + \lim_{\ell\to\infty} \frac{1}{\ell}\Psi_{w,\ell}\Phi_{\mu,\ell}^{\mathrm{T}} + \lim_{\ell\to\infty} \frac{1}{\ell}\Psi_{e_\mu,\ell}\Phi_{\mu,\ell}^{\mathrm{T}} = \lim_{\ell\to\infty} \hat{\theta}_{\mu,\ell} \lim_{\ell\to\infty} \frac{1}{\ell}\Phi_{\mu,\ell}\Phi_{\mu,\ell}^{\mathrm{T}}. \quad (37)$$

Since w is a realization of a white, zero-mean random processes and u is deterministic, then $\lim_{\ell\to\infty} \frac{1}{\ell}\Psi_{w,\ell}\Phi_{\mu,\ell}^{\mathrm{T}} = 0_{1\times\mu}$. Therefore, (37) becomes

$$\alpha\theta_\mu \lim_{\ell\to\infty} \frac{1}{\ell}\Phi_{\mu,\ell}\Phi_{\mu,\ell}^{\mathrm{T}} + \theta_\mu \lim_{\ell\to\infty} \frac{1}{\ell}\Phi_{\rho,\ell}\Phi_{\mu,\ell}^{\mathrm{T}} + \lim_{\ell\to\infty} \frac{1}{\ell}\Psi_{e_\mu,\ell}\Phi_{\mu,\ell}^{\mathrm{T}} = \lim_{\ell\to\infty} \hat{\theta}_{\mu,\ell} \lim_{\ell\to\infty} \frac{1}{\ell}\Phi_{\mu,\ell}\Phi_{\mu,\ell}^{\mathrm{T}}. \quad (38)$$

Since u is a persistently exciting signal of sufficient order, then $Q \triangleq \lim_{\ell\to\infty} \frac{1}{\ell}\Phi_{\mu,\ell}\Phi_{\mu,\ell}^{\mathrm{T}}$ has full rank. Therefore, multiplying (38) by Q^{-1} from the right yields

$$\alpha\theta_\mu + \theta_\mu RQ^{-1} + \lim_{\ell\to\infty} \frac{1}{\ell}\Psi_{e_\mu,\ell}\Phi_{\mu,\ell}^{\mathrm{T}}Q^{-1} = \lim_{\ell\to\infty} \hat{\theta}_{\mu,\ell}, \quad (39)$$

where $R \triangleq \lim_{\ell\to\infty} \frac{1}{\ell}\Phi_{\rho,\ell}\Phi_{\mu,\ell}^{\mathrm{T}}$.

Note that

$$\begin{aligned} R &= \lim_{\ell\to\infty} \frac{1}{\ell}\Phi_{\rho,\ell}\Phi_{\mu,\ell}^{\mathrm{T}} \\ &= \lim_{\ell\to\infty} \frac{1}{\ell} \begin{bmatrix} \rho(\mu) & \cdots & \rho(\ell) \\ \vdots & \ddots & \vdots \\ \rho(0) & \cdots & \rho(\ell-\mu) \end{bmatrix} \begin{bmatrix} u(\mu) & \cdots & u(0) \\ \vdots & \cdots & \vdots \\ u(\ell) & \cdots & u(\ell-\mu) \end{bmatrix} \\ &= \lim_{\ell\to\infty} \frac{1}{\ell} \begin{bmatrix} \displaystyle\sum_{j=\mu}^{\ell}\rho(i)u(i) & \cdots & \displaystyle\sum_{j=\mu}^{\ell}\rho(i)u(i-\mu) \\ \vdots & \ddots & \vdots \\ \displaystyle\sum_{j=\mu}^{\ell}\rho(i-\mu)u(i) & \cdots & \displaystyle\sum_{j=0}^{\ell-\mu}\rho(i)u(i) \end{bmatrix}. \end{aligned} \quad (40)$$

Moreover, note that

$$\begin{aligned} Q &= \lim_{\ell\to\infty} \frac{1}{\ell}\Phi_{\mu,\ell}\Phi_{\mu,\ell}^{\mathrm{T}} \\ &= \lim_{\ell\to\infty} \frac{1}{\ell} \begin{bmatrix} u(\mu) & \cdots & u(\ell) \\ \vdots & \ddots & \vdots \\ u(0) & \cdots & u(\ell-\mu) \end{bmatrix} \begin{bmatrix} u(\mu) & \cdots & u(0) \\ \vdots & \cdots & \vdots \\ u(\ell) & \cdots & u(\ell-\mu) \end{bmatrix} \\ &= \lim_{\ell\to\infty} \frac{1}{\ell} \begin{bmatrix} \displaystyle\sum_{j=\mu}^{\ell}u(i)^2 & \cdots & \displaystyle\sum_{j=\mu}^{\ell}u(i)u(i-\mu) \\ \vdots & \ddots & \vdots \\ \displaystyle\sum_{j=\mu}^{\ell}u(i)u(i-\mu) & \cdots & \displaystyle\sum_{j=0}^{\ell-\mu}u(i)^2 \end{bmatrix}. \end{aligned} \quad (41)$$

Note from (40) and (41) that if the entries of R are much smaller than the entries of Q, then RQ^{-1} can be neglected. Therefore, we choose the amplitude of the input signal u to be as large as possible. Assuming that RQ^{-1} can be neglected, (39) becomes

$$\alpha\theta_\mu + \lim_{\ell\to\infty} \frac{1}{\ell}\Psi_{e_\mu,\ell}\Phi_{\mu,\ell}^{\mathrm{T}}Q^{-1} \approx \lim_{\ell\to\infty} \hat{\theta}_{\mu,\ell}. \quad (42)$$

Note from (22) and (30) that, as μ increases, the entries of $\Psi_{e_\mu,\ell}$ become smaller. Therefore, we choose μ to be large enough such that

$$\lim_{\ell\to\infty} \frac{1}{\ell}\Psi_{e_\mu,\ell,\mu}\Phi_{u,\ell,\mu}^{\mathrm{T}} \approx 0_{1\times(\mu+1)}. \quad (43)$$

Therefore, (42) becomes

$$\lim_{\ell\to\infty} \hat{\theta}_{\mu,\ell} \approx \alpha\theta_\mu. \quad (44)$$

It follows from (44) that $\hat{\theta}_{\mu,\ell}$ is approximately a semiconsistent estimate of θ_μ, that is, $\lim_{\ell\to\infty} \hat{\theta}_{\mu,\ell}$ is a correct estimate of θ_μ up to an unknown scalar factor.

V. Identification of the Hysteresis Nonlinearity

Identification of the hysteresis nonlinearity is performed by first estimating the unknown intermediate signal v, and then using the input u and the estimated intermediate signal to construct an estimate of the hysteresis nonlinearity.

Note that, if we use y as an input to the transfer function $G^{-1} = 1/G$, then the output of G^{-1} is the unknown intermediate signal v. Assuming that $\hat{G}$ is an estimate of the transfer function G, then using y as an input to the transfer function $\hat{G}^{-1} = 1/\hat{G}$, the output of $\hat{G}^{-1}$ is an estimate $\hat{v}$ of the unknown intermediate signal v. However, if $\hat{G}$ is strictly proper, then $\hat{G}^{-1}$ is improper, that is, noncausal. Moreover, if $\hat{G}$ has a nonminimum-phase zero, that is, a zero that is outside the closed unit disk, then $\hat{G}^{-1}$ is unstable. In order to simulate $\hat{G}^{-1}$ with y as an input, we need to circumvent these two problems.

Noncausal FIR models have been used to obtain asymptotically stable approximations of unstable and noncausal systems [24]. A noncausal FIR model of a transfer function H is a truncation of the Laurent expansion of H in an annulus that contains the unit circle [24].

A. Asymptotically Stable Inversion of G

Let $\mathbb{A}(\rho_1,\rho_2) \triangleq \{z \in \mathbb{C} : |z| > \rho_1 \text{ and } |z| < \rho_2\}$ denote an open annulus in the complex plane centered at the origin with inner radius ρ_1 and outer radius ρ_2, where $\rho_1 < 1 < \rho_2$. Then, the Laurent expansion of $\hat{G}^{-1}$ in $\mathbb{A}(\rho_1,\rho_2)$ can be written as

$$\hat{G}^{-1}(z) = \sum_{i=-\infty}^{\infty} \hat{h}_i z^{-i}, \quad (45)$$

where $\hat{h}_i$ is the ith coefficient of the Laurent expansion of $\hat{G}^{-1}$ in $\mathbb{A}(\rho_1,\rho_2)$. Truncating the sum in (45) yields the truncated model

$$\hat{G}_{\mathrm{inv},r,d}(\mathbf{q}) \triangleq \sum_{i=-d}^{r} \hat{h}_i \mathbf{q}^{-i}, \quad (46)$$

where r is the order of the causal part of $\hat{G}_{\mathrm{inv},r,d}$ and d is the order of the noncausal part of $\hat{G}_{\mathrm{inv},r,d}$. Note that all

poles of $\hat{G}_{\mathrm{inv},r,d}$ are located at zero, and thus $\hat{G}_{\mathrm{inv},r,d}$ is an asymptotically stable approximation of $\hat{G}^{-1}$. Assuming that $\hat{G}^{-1}$ has no poles on the unit circle, then we can find finite r and d such that the $\|\hat{G}^{-1} - \hat{G}_{\mathrm{inv},r,d}\|$ is negligible [24, Theorem 4.1], [27].

Using y as an input to $\hat{G}_{\mathrm{inv},r,d}$, and using (46), yields, for all $k \geq r$,

$$\hat{v}(k) = \hat{G}_{\mathrm{inv},r,d}(\mathbf{q})y(k) = \sum_{i=-d}^{r} \hat{h}_i y(k-i). \qquad (47)$$

Note from (47) that computing $\hat{v}(k)$ requires knowledge of $y(k+d), \ldots, y(k-r)$, which makes $\hat{G}_{\mathrm{inv},r,d}$ noncausal.

B. Identification of the Hysteresis Nonlinearity

To obtain the shape of the hysteresis loop, we run the Hammerstein system with a new input signal, u, which is a single sinusoidal signal with a specific frequency. Then, we use the output of the Hammerstein system due to u and $\hat{G}_{\mathrm{inv},r,d}$ obtained from the previous subsection to construct an estimate $\hat{v}$ of the intermediate signal v. Then, we plot $\hat{v}$ versus u to obtain a nonparametric model of the hysteresis nonlinearity. If the hysteresis nonlinearity is rate independent, then the estimated hysteresis nonlinearity is independent of the frequency of the single sinusoidal input.

C. Numerical Example

Consider the piezoceramic actuator described in [28], which is characterized by the transfer function

$$G(s) = \frac{3.391 \times 10^{10}}{s^3 + 3759s^2 + 2.063 \times 10^7 s + 7.514 \times 10^{10}} \qquad (48)$$

and the GPI hysteresis model described by $r_1 = 0.0769$, $r_2 = 0.1538$, $r_3 = 0.2307$, $r_4 = 0.3076$, $r_5 = 0.3845$, $r_6 = 0.4614$, $r_7 = 0.5383$, $r_8 = 0.6152$, $p_1 = 3.6590$, $p_2 = 2.8098$, $p_3 = 2.1577$, $p_4 = 1.6569$, $p_5 = 1.2724$, $p_6 = 0.9771$, $p_7 = 0.7503$, $p_8 = 0.5762.$, $\eta_1 = -6.4$, $\eta_2 = -5.6$, $\eta_3 = -4.8$, $\eta_4 = -4.0$ $\eta_5 = -3.2$, $\eta_6 = -2.4$, $\eta_7 = -1.6$, $\eta_8 = -0.8$, $\eta_9 = 0$, $\eta_{10} = 0.8$, $\eta_{11} = 1.6$, $\eta_{12} = 2.4$, $\eta_{13} = 3.2$, $\eta_{14} = 4.0$, $\eta_{15} = 4.8$, $\eta_{16} = 5.6$, $\eta_{17} = 6.4$, $g_1 = -0.198$, $g_2 = -0.057$, $g_3 = -0.1669$, $g_4 = -0.13$, $g_5 = -0.15$, $g_6 = -0.037$, $g_7 = 0.02$, $g_8 = 0.23$, $g_9 = 0$, $g_{10} = -0.249$, $g_{11} = -0.004$, $g_{12} = -0. - 0.2176$, $g_{13} = -0.0734$, $g_{14} = 0.0568$, $g_{15} = -0.058$, $g_{16} = -0.13$, $g_{17} = -2.479$.

For all $k \geq 0$, let $u(k) = \sum_{i=1}^{1000} 5\sin(\omega_i T_{\mathrm{s}} k)$, where for all $i = 1, \ldots, 1000$, $\omega_i = i$. We consider the sampling time of $T_{\mathrm{s}} = 1 \times 10^{-5}$ sec. Then

$$G(z) = \frac{0.256z^2 + 0.02439z + 0.1349}{z^3 - 0.5746z^2 + 0.4949z - 9.137 \times 10^{-17}}. \qquad (49)$$

To identify G, we consider u and y with least squares and an FIR model with order $\mu = 30$ and $\ell = 100,000$ data samples. Figure 3 shows the Markov parameters of G and the estimated Markov parameters of G after scaling. Then, we construct an IIR model $\hat{G}$ of G using ERA and the estimated Markov parameters of G after scaling. Figure 4 shows the Bode plot of G and $\hat{G}$. We apply y as an input

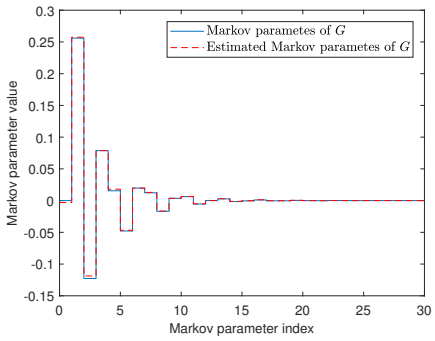

Fig. 3. Markov parameters of G and the estimated Markov parameters of G after scaling.

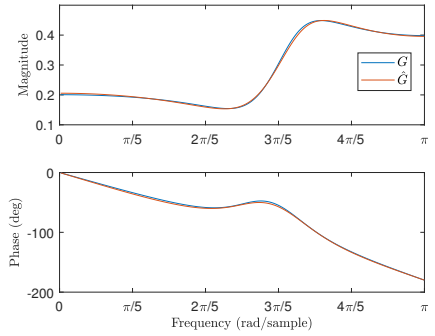

Fig. 4. Bode plot of G and the identified model $\hat{G}$ after scaling.

to the noncausal FIR approximation $\hat{G}_{\mathrm{inv},r,d}$ of $\hat{G}^{-1}$. Figure 5 shows the intermediate signal v and the estimate $\hat{v}$ of v, obtained by applying y as an input to the noncausal FIR approximation $\hat{G}_{\mathrm{inv},r,d}$ of $\hat{G}^{-1}$. Next, suppose that for all $k \geq 0$, $u(k) = 10\sin(T_{\mathrm{s}}k)$. We use the output y due to the sinusoidal input u and the noncausal FIR approximation of $\hat{G}^{-1}$ to estimate the unknown intermediate signal $\hat{v}$ due to the sinusoidal input u. Figure 6(top) shows the intermediate signal v and the estimate $\hat{v}$ of v, obtained by applying y as an input to the noncausal FIR approximation $\hat{G}_{\mathrm{inv},r,d}$ of $\hat{G}^{-1}$. Moreover, Figure 6(bottom) shows the hysteresis loop obtained using u and v and the estimated hysteresis loop obtained using u and $\hat{v}$.

VI. Conclusions

In this paper, we presented an algorithm to identify nonlinear dynamics in piezomicropositioning actuators, which are modeled as Hammerstein systems, i.e. a cascade of a GPI hysteresis nonlinearity and a linear dynamic system. Least squares with an FIR model were used to identify the linear plant using the input and output of the Hammerstein system. The ERA algorithm was used to construct a transfer function model from the estimated FIR model. A noncausal FIR model was used to obtain an asymptotically stable approximation of the inverse of the estimated linear part, which was used along with the output of the Hammerstein system to obtain an estimate of the unknown intermediate signal. Finally, the input to the Hammerstein system and the estimate of the intermediate signal were used to obtain an estimate of the hysteresis nonlinearity.

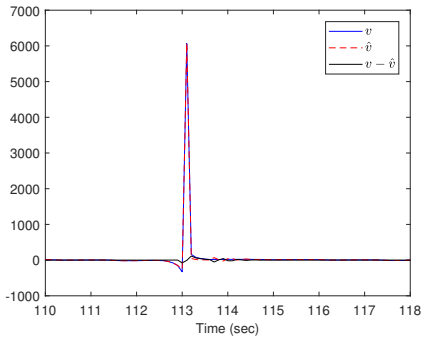

Fig. 5. Plot of the intermediate signal v and the estimate $\hat{v}$ obtained by applying y as an input to the noncausal FIR approximation $\hat{G}_{\mathrm{inv},r,d}$ of $\hat{G}^{-1}$.

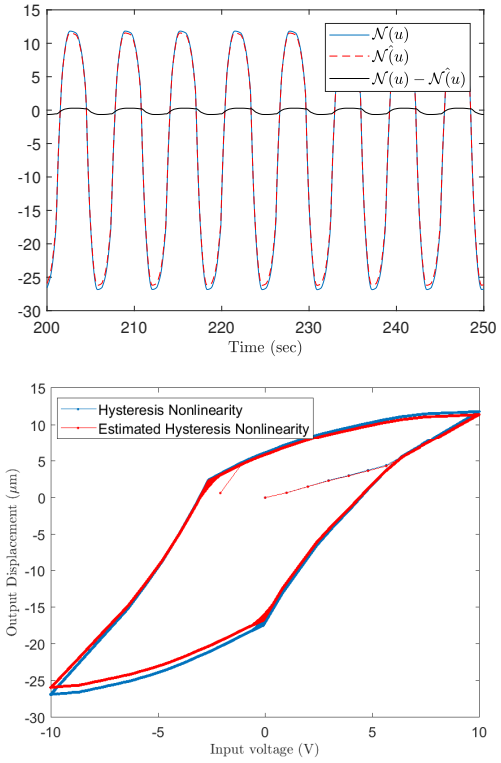

Fig. 6. (Top) Intermediate signal v and estimated intermediate signal $\hat{v}$ obtained by applying y as an input to the noncausal FIR approximation $\hat{G}_{\mathrm{inv},r,d}$ of $\hat{G}^{-1}$, where for all $k \geq 0$, $u(k) = \sin(T_{\mathrm{s}}k)$. (Bottom) Hysteresis loop obtained by plotting v versus u and estimated hysteresis loop obtained by plotting $\hat{v}$ versus u.

REFERENCES

[1] J. Agnus, "Robotic microassembly and micromanipulation at femto-st," *Journal of Micro-Bio Robotics*, pp. 91–106, 2013.

[2] L. Fang, J. Wang, and X. Tan, "An incremental harmonic balance-based approach for harmonic analysis of closed-loop systems with Prandtl-Ishlinskii operator," *Automatica*, pp. 48–56, 2018.

[3] M. Butcher, A. Giustiniani, and A. Masi, "On the identification of Hammerstein systems in the presence of an input hysteretic nonlinearity with nonlocal memory: Piezoelectric actuators an experimental case study," *Physica B*, vol. 486, pp. 101–105, 2016.

[4] M. Rakotondrabe, "Multivariable classical prandtl-ishlinskii hysteresis modeling and compensation and sensorless control of a nonlinear 2-dof piezoactuator," *Nonlinear Dynamics*, 2017.

[5] X. Tan and J. Baras, "Modeling and control of hysteresis in magnetostrictive actuators," *Automatica*, vol. 40, pp. 1469–1480, 2004.

[6] M. Edardar, X. Tan, and H. Khalil, "Design and analysis of sliding mode controller under approximate hysteresis compensation," *IEEE Transactions on Control Systems Technology*, pp. 48–56, 2015.

[7] M. AlJanaideh, M. Rakotondrabe, I. Al-Darabsah, and O. Aljanaideh, "Internal model-based feedback control design for inversion-free feedforward rate-dependent hysteresis compensation of piezoelectric cantilever actuator," *Control Engineering Practice*, vol. 72, 2018.

[8] M. AlJanaideh, S. Rakheja, and C.-Y. Su, "An analytical generalized prandtl-ishlinskii model inversion for hysteresis compensation in micropositioning control," *IEEE/ASME Transactions on Mechatroncis*, vol. 16, pp. 734–744, 2011.

[9] D. Davino, C. Natale, S. Pirozzi, and C. Visone, "Phenomenological dynamic model of a magnetostrictive actuator," *Physica B: Condensed Matter*, vol. 343, pp. 112–116, 2004.

[10] J. Schoukens, J. Nemeth, P. Crama, Y. Rolain, and R. Pintelon, "Fast approximate identification of nonlinear systems." *Automatica*, vol. 39, pp. 1267–1274, 2003.

[11] T. H. Van Pelt and D. S. Bernstein, "Non-linear system identification using Hammerstein and non-linear feedback models with piecewise linear static maps." *International Journal of Control*, vol. 74, pp. 1807–1823, 2001.

[12] B. Ninness and S. Gibson, "Quantifying the accuracy of Hammerstein model estimation." *Automatica*, vol. 38, pp. 2037–2051, 2002.

[13] E.-W. Bai, "Identification of linear systems with hard input nonlinearities of known structure," *Automatica*, vol. 38, pp. 853–860, 2002.

[14] F. Ding, X. P. Liu, and G. Liu, "Identification methods for Hammerstein nonlinear systems," *Digital Signal Processing*, vol. 21, no. 2, pp. 215–238, 2011.

[15] K. F. Aljanaideh and D. S. Bernstein, "Nonparametric identification of Hammerstein systems using orthogonal basis functions as ersatz nonlinearities," in *ASME Dynamic Systems Control Conference*, 2013, p. V003T35A004.

[16] B. J. Coffer, K. Aljanaideh, and D. S. Bernstein, "Identification of Hammerstein systems using input amplitude multiplexing," in *American Control Conference*, 2013, pp. 3930–3935.

[17] F. Giri, Y. Rochdi, F. Chaoui, and A. Brouri, "Identification of Hammerstein systems in presence of hysteresis-backlash and hysteresis-relay nonlinearities," *Automatica*, vol. 44, no. 3, pp. 767–775, 2008.

[18] H. V. H. Ayala, D. Habineza, M. Rakotondrabe, C. E. Klein, and L. S. Coelho, "Nonlinear black-box system identification through neural networks of a hysteretic piezoelectric robotic micromanipulator," *IFAC Symposium on System Identification*, pp. 409–414, 2015.

[19] K. F. Aljanaideh, M. Rakotondrabe, M. Al Janaideh, and D. Kundur, "Identification of precision motion systems with Prandtl-Ishlinskii hysteresis nonlinearities," *Proc. American Control Conference*, pp. 5225–5230, 2018.

[20] A. Cavallo, D. Davino, G. D. Maria, C. Natale, S. Pirozzi, and C. Visone, "Hysteresis compensation of smart actuators under variable stress conditions," *Physica B: Condensed Matter*, vol. 403, 2008.

[21] K. Leang and S. Devasia, "Feedback-linearized inverse feedforward for creep, hysteresis, and vibration compensation in afm piezoactuators," *IEEE Transactions on Control Systems Technology*, vol. 15, pp. 927–935, 2007.

[22] M. Rakotondrabe, "Modeling and compensation of multivariable creep in multi-dof piezoelectric actuators," *IEEE International Conference on Robotics and Automation*, pp. 4577–4581, 2012.

[23] M. A. Janaideh and O. Aljanaideh, "Further results on open-loop compensation of rate-dependent hysteresis in a magnetostrictive actuator with the prandtl-ishlinskii model," *Mechanical Systems and Signal Processing*, vol. 104, pp. 835–850, 2018.

[24] K. F. Aljanaideh and D. S. Bernstein, "Closed-loop identification of unstable systems using noncausal FIR models," *International Journal of Control*, vol. 90, no. 2, pp. 168–185, 2017.

[25] J.-N. Juang, *Applied system identification*. Prentice Hall, 1994.

[26] B. Ho and R. Kalman, "Efficient construction of linear state variable models from input/output functions," *Regelungstechnik*, vol. 14, pp. 545–548, 1966.

[27] D. S. Bernstein, K. F. Aljanaideh, and A. E. Frazho, "Laurent series and ℓ^p sequences," *American Mathematical Monthly*, vol. 123, pp. 398–398, 2016.

[28] Y. Shan and K. Leang, "Design and control for high-speed nanopositioning: serial-kinematic nanopositioners and repetitive control for nanofabrication," *IEEE Control Systems Magazine*, vol. 33, pp. 86–105, 2013.